From: "From Solar Min to Max: Half a solar cycle with SoHO", Proc. SoHO 11 Symposium, Davos, Switzerland, March 2002, ESA-SP-508, pp 507- 522, ESA Publications, Noordvijk, The Netherlands, 2002

LONG-TERM VARIATIONS IN THE OPEN SOLAR FLUX AND POSSIBLE LINKS TO EARTH'S CLIMATE

M. Lockwood [1, 2]
[1] Rutherford Appleton Laboratory, Space Science and Technology Department, Chilton, Oxfordshire, OX11 0DQ, U.K.
(tel. +44-1235-446496; fax. +44-1235-445848; e-mail m.lockwood@rl.ac.uk)
[2] Southampton University, Department of Physics and Astronomy, Southampton, Hampshire, SO17 1BJ, U.K.

ABSTRACT

Recent paleoclimate studies provide strong evidence for an association between cosmogenic isotope production and Earth's climate throughout the holecene. These isotopes are generated by the bombardment of Earth's atmosphere by galactic cosmic rays, the fluxes of which vary in approximately inverse proportion to the total open magnetic flux of the Sun. This paper discusses how results from the Ulysses spacecraft allow us to quantify the open solar flux from observations of near-Earth interplanetary space and to study its long-term variations using the homogeneous record of geomagnetic activity. A study of the results and of their accuracy is presented. The two proposed mechanisms that could lead to the open solar flux being a good proxy for solar-induced climate change are discussed: the first is the modulation of the production of some types of cloud by the air ions produced by cosmic rays; the second is a variation in the total or spectral solar irradiance, in association with changes in the open flux. Some implications for our understanding of anthropogenic climate change are discussed.

Key words: Solar variability; climate change; heliospheric field; solar irradiance; galactic cosmic rays; cosmogenic isotopes

1. INTRODUCTION

1.1. Open Solar Flux and Climate

There have been a number of recent studies which have linked changes in the abundance of deposited cosmogenic isotopes with climate variations throughout the holocene (the current warm period between ice ages caused by the Milankovitch cycles of Earth's orbit and precession). A review of this research has been presented by *Kirkby* [2001]: we here illustrate the implications by reference to just one of these studies. *Bond et al.* [2001] have investigated the abundance of "ice-rafted debris" in deep-sea sediments, as measured in ocean-bed cores taken from throughout the mid-latitude and north Atlantic. This debris consists of petrologic tracers (specifically, hematite-stained grains, Icelandic glass, and detrital carbonate) whose origins can be traced to glaciers in known locations. They are carried by icebergs and deposited in the sediment as the ice melts. The abundances of the tracers in the sediments at given locations are sensitive indicators of the amounts and trajectories of glacial and sea ice and thus of the surface winds, currents and temperature throughout the sub-polar Atlantic. By dating the sediment layers, *Bond et al.* find highly significant correlations with cosmogenic isotopes. These isotopes are produced as spallation products when galactic cosmic rays interact with atmospheric nitrogen, oxygen and argon nucleii. The isotopes with the highest production rates are ^{14}C (global mean production rate of order 2 atoms $cm^{-2}s^{-1}$ and half life of 5730 ± 40 yrs) and ^{10}Be (global mean production rate of order 0.018 atoms $cm^{-2}s^{-1}$ and half life of 1.5×10^{6} yrs). The ^{14}C is absorbed as CO_2 gas by organic material with the prevailing atmospheric fraction, and this subsequently decays with the ^{14}C characteristic half life. Thus the abundance found in ancient trees, such as Californian Bristlecone pines, can give the atmospheric abundance, dated by counting the tree rings reflecting the annual growth cycle. The ^{10}Be is attached to aerosols and circulates in the atmosphere. That produced in the stratosphere (about 2/3 of the total) takes of order 1-2 years to precipitate to Earth's surface, the corresponding time for the other 1/3 produced in the troposphere is only about 1 week. This ^{10}Be is found in ice sheets precipitated as snowflakes before being compacted and can, in principle, be dated by counting the layers of ice reflecting the annual cycle of local weather. (In practice, the dating requires careful modelling of the ice sheet flow). *Bond et al.* find a correlation of the average abundance of the ice rafted debris of 0.44 with the production rate of ^{14}C and of 0.56 with ^{10}Be abundance.

The fact that these correlations are found for both the ^{14}C and ^{10}Be cosmogenic isotopes is significant [*Bard et al.*, 1997]. Because these cosmogenic isotopes are produced in the atmosphere, their production and deposition of could depend on climate. The ^{10}Be remains in the atmosphere until it is precipitated into the ice sheet. On the other hand, ^{14}C is absorbed in the gaseous state but is also stored in the vast reservoir of Earth's oceans as well as in the biomass. The exchange of ^{14}C between the atmosphere and these other two reservoirs needs to be accounted for before the primary production rate by cosmic rays can be estimated from the abundance of the ^{14}C isotope. Thus in both cases, if taken individually, Earth's climate could potentially have influenced the production and deposition of the isotope and so influenced the correlation. However, the deposition of the two isotopes is so vastly different that this cannot be a viable explanation of the observation that both the isotopes correlate with the ice-rafted debris. The one common denominator for the two isotopes is production by the flux of primary cosmic rays

impacting upon Earth's atmosphere. Thus it is deduced that the long-term climate variations throughout the holocene correlate well with the fluxes of galactic cosmic rays [*Beer*, 2000]. In section 3 we will discus how these fluxes are related to the open solar magnetic flux that fills the heliosphere.

If these correlations are genuine, and the above reasoning concerning any potential effects of climate on the deposition is correct, one is left with one of two viable alternatives (or a combination of them). Both are remarkable and controversial, and either would have far-reaching implications.

The first possibility is that the galactic cosmic rays influence Earth's climate directly. One such effect has been proposed by Henrik Svensmark and co-workers from observations showing an apparent solar cycle variation in global cloud cover [*Svensmark and Friis-Christensen*, 1997; *Svensmark*, 1998; *Marsh and Svensmark*, 2000a; b]. This variation is largely seen for low-altitude clouds in maritime regions and is discussed further in section 4.1. It is often said that there is no viable microphysical mechanism whereby cloud production can be modulated by cosmic rays. Such statements ignore the theoretical and experimental studies that provide a variety of possible mechanisms for the production of cloud condensation nuclei from the air ions generated by galactic cosmic rays [*Yu and Turco*, 2000; *Harrison and Alpin*, 2001; *Kirkby* 2001 and references therein]. A far more relevant question is "are the mechanisms that have been proposed for ion-induced nucleation efficient enough to have any significant effect in relation to the many other sources of cloud cover?"

The second possibility is that the cosmic rays which generate the cosmogenic isotopes are highly correlated with another factor that influences climate (such that the cosmic rays and the isotopes that they produce are valuable proxies for that factor). *Lockwood and Stamper* [1999] noted that the total open flux of the Sun shows a very good correlation with the measured total solar irradiance (TSI) – the total power of electromagnetic radiation received per unit area at the Earth. Recently, *Lockwood* [2002a] has shown that this correlation is maintained in the most recent TSI data from the SoHO spacecraft. A change in the TSI will influence Earth's climate and it is interesting to note that the paleoclimate scientists regard the cosmogenic isotopes as proxy indicators of the TSI – in other words they tacitly assume the correlations found by *Lockwood and Stamper* and *Lockwood*. However, cosmic ray fluxes are really indicators of heliospheric shielding, and in section 3 we show that most of their variation, at least on timescales exceeding one year, is anticorrelated with the open solar flux in the heliosphere. *Lockwood* [2002a] has directly studied the anticorrelations between cosmic ray fluxes and TSI and shown that they are statistically very significant. But this raises important questions about the Sun and the origin of the TSI variations. We lack an explanation as to why the open solar flux might be a good indicator of the TSI on a range of timescales. *Lockwood and Stamper* and *Lockwood* have shown that open flux, cosmic rays and TSI are closely related over recent 11-year solar cycles. However, without a physical understanding of this relationship, we cannot tell whether or not it also applies over the 100-year Gleissberg cycles of solar activity [*Gleissberg*, 1944], relevant to modern global warming studies, let alone on the timescales of the fluctuations (period ~1500 years) seen throughout the holocene [e.g. *Bond et al*., 2001].

1.2. Quantifying the Open Solar Flux

The open magnetic flux of the Sun has been estimated in two ways. The first is from surface magnetograms which give the line-of-sight component of the photospheric magnetic field. This is mapped up to a hypothetical surface called the "coronal source surface" where the field is purely radial. In order to do this, it is usually assumed that there are no currents in the corona between the photosphere and the source surface. The source surface is also usually assumed to be spherical at a heliocentric distance of $r = 2.5R_s$ (where a mean solar radius, $1R_s = 6.96\times10^8$ m). Although a very useful idealised concept, there is no apriori reason why this surface should be spherical – indeed it may not exist at all. Thus although the "potential field source surface" (PFSS) methods which make use this concept [*Schatten et al.*, 1969; *Schatten*, 1999; *Wang and Sheeley*, 1995] give a useful indication of the distribution of the photospheric footprints of the open flux, there are uncertainties concerning the quantification of the total open flux by this method because of the assumptions involved.

The second, more direct, method for computing open flux has been made possible by the discovery by the Ulysses spacecraft that the radial component of the heliospheric field is independent of heliographic latitude [*Balogh et al*., 1995; *Lockwood et al*., 1999b; *Smith et al*. 2001]. This means that there are sheet currents, but no volume currents in the heliosphere. This discovery has been explained in terms of the low plasma β of the expanding solar wind at about $1.5R_s < r < 10R_s$, where non-radial flow allows the magnetic flux to re-distribute itself to give latitude independent tangential magnetic pressure and thus a uniform radial field component [*Suess and Smith*, 1996; *Suess et al*., 1996].

Because of this result, the radial field seen near Earth B_{r1} can be used to compute the total (signed) flux threading a heliocentric sphere of radius R_1 = 1 AU (1AU is the mean Earth-Sun distance, 150×10^6 km):

$$F_S' = 4\pi R_1^2 |B_{r1}| / 2 \qquad (1)$$

The factor 2 arises because half the flux through this surface is outward and half is inward. Section 2.1 analyses the errors introduced by the use of equation (1). We here use the prime to denote that the open flux is

estimated assuming the Ulysses result that the radial field is independent of latitude.

The two methods can be made to yield consistent results. However, in order to achieve this, *Wang and Sheeley* [1995] found an improved, latitude-dependent line saturation correction factor must be applied to the photospheric field data. With this, these authors were able to match to the radial field seen at Earth during solar cycles 20 and 21, again using the assumption that B_r is independent of latitude in the heliosphere. Recent work by *Wang and Sheeley*. [2002] shows that the two methods are also in good general agreement for the more recent data from cycles 22 and 23.

There is one additional difference between the two methods. The PFSS methods quantify the open flux threading the coronal source surface (usually assumed to be at $r = 2.5R_s$). On the other hand, the near-Earth method quantifies the flux threading a fixed heliocentric sphere at $r = R_1$. From flux transport over IMF monitors during the solar wind transit times from $r = 2.5R_s$ to $r = R_1$, *Lockwood* [2002b] has quantified the open flux F_o which threads the assumed coronal source surface ($r = 2.5R_s$) but which closes in the inner heliosphere, such that it does not thread the spherical surface at $r = R_1$. The results for hourly data show symmetric distributions of F_o about zero, with upper and lower deciles of $\pm 0.2F_S'$. The uncertainty associated with such flux averages to very small values on longer timescales ($\pm 0.02F_S'$ in annual means).

2. IMPLICATIONS OF THE ULYSSES RESULT

2.1. The Uncertainty in Open Flux Estimates

The dashed line in Figure 1 shows the percentage deviation of the distance-corrected modulus of the radial field seen at Ulysses $\{(r_U/R_1)^2|B_{rU}|\}$ from that observed by near-Earth satellites $|B_{r1}|$. These data are for the first perihelion pass, which took place between day 280 of 1994 and day 235 of 1995. The heliocentric distance of the craft r_U varied from about 2.3AU at the highest latitudes down to 1.34AU at perihelion. The radial field seen by Ulysses has been corrected by the $(r_U/R_1)^2$ factor to allow for the dependence of flux tube area on r. In addition, the time δt for the solar wind observed by Ulysses to have propagated from $r = R_1$ to the satellite at $r = r_U$ has been calculated from the solar wind speed observed at Ulysses: Ulysses magnetometer observations at time t_u are then compared with near-Earth IMF data recorded at time ($t_u - \delta t$). Figure 1, from *Lockwood et al*. [2002], shows the fractional deviation of the lagged, range-corrected, averaged radial field seen by Ulysses as a function of the averaging timescale employed, T. It can be seen that in daily values, the average deviation is almost 50%, but this falls to near 10% for 27-day averages and converges with increasing T to an asymptotic limit (shown by the horizontal dashed line) of 7% for the entire pole-to-pole pass (which lasts almost twelve 27-day solar rotation periods).

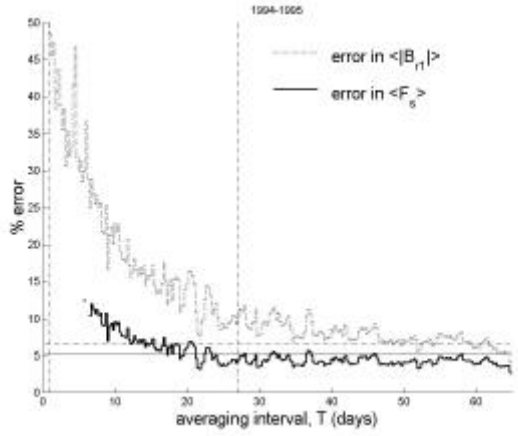

Figure 1*. Analysis of errors for the first perihelion pass of Ulysses. The dotted line gives the percent deviation of the radial field seen at Earth and at Ulysses (range corrected and lagged by the propagation time from R_1 to r_U), 100 $[(r_U/R_1)^2|B_{rU}| - |B_{r1}|] / |B_{r1}|$. The solid line is the consequent error in using equation (1) to quantify the open solar flux [from Lockwood et al. 2002].*

However, this deviation is not the error incurred in using equation (1). The total open flux is the integral of $\underline{B}.\underline{da}$ over a whole sphere (where $\underline{da}$ is a surface area element). For averaging intervals of T this becomes the sum over $N_\phi = (\tau/T)$ solar longitude bins ($\Delta\phi = 2\pi/N_\phi$ in extent) and $N_\lambda = (T_p/T)$ solar latitude bins (of roughly constant extent $\Delta\lambda = \pi/N_\lambda$), where τ is the solar rotation period and T_p is the duration of the pole-to-pole pass. Expressing the real total open flux as a fraction of that deduced from equation (1) this yields:-

$$F_S/F_S' = (1/2\pi)\sum^{N_\phi}\sum^{N_\lambda} (r_U/R_1)^2\{|B_{rU}|/|B_{r1}|\}\cos\lambda\ \Delta\lambda\Delta\phi \quad (2)$$

From equation (2) we can compute the effect of the uncertainty in $\{(r_U/R_1)^2|B_{rU}|/|B_{r1}|\}$ (given by the dotted line in figure 1) in giving an uncertainty in (F_S/F_S') and hence F_S'. The result, as a function of the averaging timescale T, is the solid line in figure 1. The important result is that the error in F_S' is less than 5% for $T \geq 27$ days. *Lockwood et al.* [2002] show that an almost identical result is obtained for the second perihelion pass of Ulysses which took place between day 353 of 2000 and day 301 of 2001. The mean sunspot numbers for these two passes were 23.5 and 106.5: thus it has been shown that the error in using equation (1) is <5% for T ≥ 27 days, at both at sunspot minimum and at sunspot maximum.

2.2. The Open Solar Flux from IMF data

Observations of the interplanetary magnetic field (IMF) have been made since 1963. The earlier data were intercalibrated into the homogeneous "Omintape" dataset of hourly data by *Couzens and King* [1986], and this has been extended with data for up to the present day.

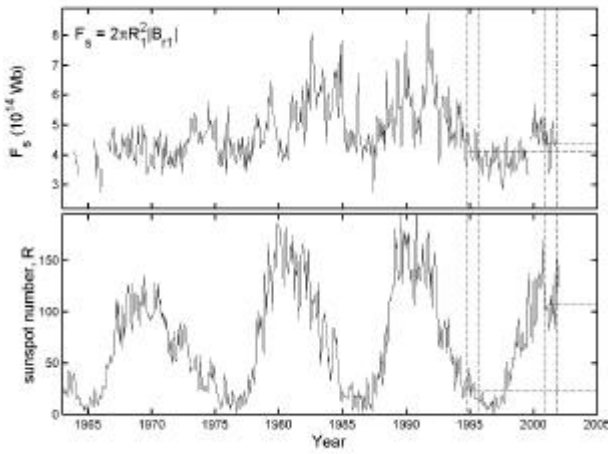

Figure 2*. The variations monthly means of (top) the open solar flux deduced from IMF observations F_s = $2p\ R_1^2|B_{r1}|$ (where R_1 = 1AU and B_{r1} is the near-Earth radial component of the IMF) and (bottom) of the sunspot number R. The vertical dashed lines mark the fast latitude scans of the first and second perihelion passes of Ulysses. The horizontal dashed lines in each panel show the mean values during these passes*

This dataset gives the near-Earth heliospheric radial field component B_{r1} which can be used with equation (1) to give the open flux estimate F_S'. To within the 5% uncertainty discussed in the previous section, F_S' is the same as F_S and hereafter we no longer make the distinction between the two.

Figure 2 shows that the open solar flux has not been constant for the past 3½ sunspot cycles. For cycle 22 the maximum-to-minimum ratio is greater than 2. Furthermore, there are long-term trends in the data which are discussed in section 2.4. The vertical dashed lines give the times of the two perihelion passes of Ulysses. The horizontal dashed lines in the top panel show the total radial flux (integrated from pole-to-pole and r^2 corrected to R_1) seen by Ulysses during these passes, $[F_S]_{U1} = 4.12\times10^{14}$ and $[F_S]_{U2} = 4.36\times10^{14}$ Wb. The horizontal dashed lines in the bottom panel show the mean sunspot numbers for these passes which were 23.5 and 106.5. Thus although the two Ulysses passes took place at very different sunspot numbers, they yielded similar open flux estimates. This is consistent with the time variation of F_S shown, which reveals that cycle 23, like cycle 20, has a small amplitude variation in F_S but that cycles 21 and 22 showed larger variations.

2.3. The aa Geomagnetic Activity Index

Mayaud [1972] devised the aa index to quantify geomagnetic activity from a data series that extend homogeneously and continuously back to 1868. On annual timescales, the aa index is almost identical to other planetary indices of geomagnetic activity derived from a greater number of stations (for example the Ap index, which is available for 1936 onwards). The aa index is generated from measurements from stations in southern England and in Australia. The variation of the annual means of aa shows two striking features. The first is the expected solar cycle variation, the second is a clear upward drift throughout the 20th century. *Clilverd et al.* [1998] made a comprehensive study of all the possible causes of this long-term drift and, by a process of elimination, concluded it was caused by a variation in interplanetary space and thus the Sun.

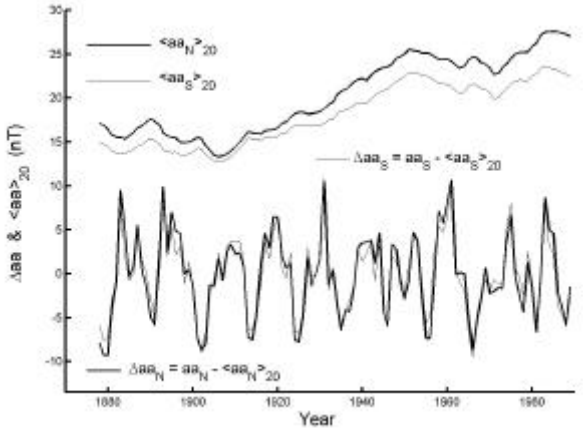

Figure 3. *The aa indices from the northern (thick lines) and southern (thin lines) hemispheres. The top pair of lines are 20-year running means, $<aa_N>_{20}$ and $<aa_S>_{20}$ revealing the long-term drifts in both the northern and southern datasets. The lower curves show the de-trended solar cycle variations in annual means $Daa_N = aa_N - <aa_N>_{20}$ and $Daa_S = aa_S$*

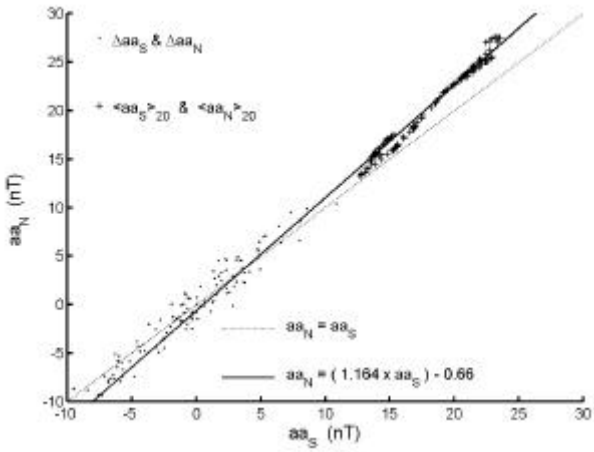

Figure 4*. Scatter plots of the aa indices from the northern and southern hemisphere. The crosses are for 20-year running means, $<aa_N>_{20}$ and $<aa_S>_{20}$. The points are for the de-trended annual means, $Daa_N = aa_N - <aa_N>_{20}$ and $Daa_S = aa_S - <aa_S>_{20}$. The solid line is the best fit to the 20-year means*

We get an indication of the solar origin of the drift if we consider how the aa index is derived. The range of horizontal perturbations to the geomagnetic field in every 3-hour interval is scaled and converted into an aa index for each hemisphere (aa_N and aa_S) using the sta-

tion-dependent scaling procedure devised by *Mayaud* [1972]. Figure 3 presents the 20-year running means, $<aa_N>_{20}$ and $<aa_S>_{20}$ which show the long-term drift is present in both the northern and southern hemisphere data and has an almost identical waveform in the two cases. However, the drift is consistently 16% larger in amplitude for the northern hemisphere. Figure 3 also gives the de-trended solar cycle variations in annual means $\Delta aa_N = aa_N - <aa_N>_{20}$ and $\Delta aa_S = aa_S - <aa_S>_{20}$. The two show very similar solar cycle variations. Figure 4 is a scatter plot of the northern and southern hemisphere data, the points being for the detrended solar cycle variations, the crosses being for the running means. The solid line is a best-fit linear regression to the 20-year means and has a slope of 1.16. This regression line also matches the detrended data well, i.e. the solar cycle variation also shows the northern hemisphere data to be consistently 16% larger in amplitude than the southern. If the scaling factors (for converting the ranges observed at the two stations into hemispheric aa indices) were perfect, this regression fit would be the dotted line of slope 1 shown in figure 4. The fact that both the solar cycle variation and the long-term drift lie on the same line strongly suggests that the long-term drift and the solar cycle share the same cause, i.e. the Sun. This also confirms *Clilverd et al.*'s elimination of several possibilities that would have influenced the ratio of the station-dependent scaling factors. For example, the change in Earth's magnetic axis has caused drifts in the geomagnetic latitudes of the northern and southern hemisphere stations which are in opposite directions. The conclusion that the drift is due to a solar effect is confirmed and quantified by the analysis of *Stamper et al.* [1999] *and Lockwood et al.* [1999a] have presented a method for computing the radial component of the near-Earth IMF from annual means of the aa geomagnetic activity index. The Ulysses result can then be applied, as in section 2.2, to give the open flux variation over the longer period covered by homogeneous observations of geomagnetic activity.

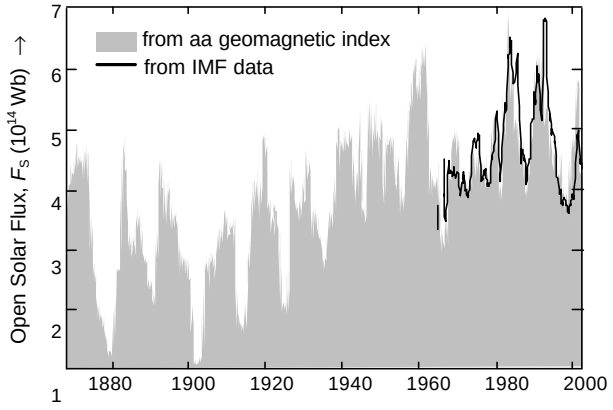

***Figure 5**. The variations of open solar flux. The area shaded grey gives values for one year (advanced by one month at a time) derived from the aa geomagnetic index, the black solid line gives monthly values from IMF observations (shown in more detail in the top panel of figure 2).*

al. [1999a], discussed in the next section.

2.4. The Open Solar Flux from Geomagnetic Activity

A description of the procedure has been given previously [*Lockwood et al*., 1999a; b, *Lockwood and Stamper*, 1999] and will not be repeated here. However, there are some important points to stress because the method is physics-based and is far from being a simple statistical extrapolation using a fit to the aa index. Firstly, it is based on the theory of solar-wind magnetosphere energy coupling by *Vasyluinas et al.* [1982], which has been shown to be the most successful by *Finch et al.* [2002], giving a correlation of 0.97 between interplanetary parameters and the aa index on annual timescales. Secondly, it employs the Parker spiral theory to the ecliptic heliospheric field which, on the annual timescales used, matches the data exceptionally well [*Gazis*, 1996; *Stamper et al*., 1999]. Thirdly, the method exploits our understanding of the role of fast solar wind streams (from long-lived low-latitude coronal holes) in generating recurrent geomagnetic activity [*Cliver et al*., 1996; *Hapgood*, 1994] this enables us to remove the effect of solar wind velocity variations. The three correlations used to generate the required coefficients are all over 0.95 and are all more than 99.999% significant, allowing for the persistence in the various data series. The results for 1868-2001 are shown in figure 5 and compared with the open flux from the near-Earth IMF observations.

2.5. The Long-Term Variation of the Open Solar Flux

Figure 6 shows 11-year running means of the open solar flux. Values derived from aa reveal that the average increased by a factor of about 2 during the 20th century.

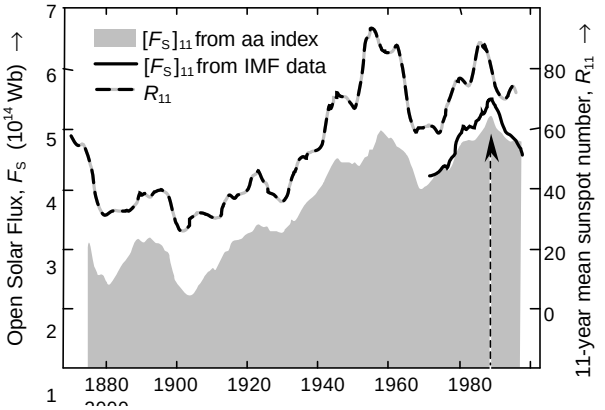

***Figure 6.** Variations in solar cycle means. The area shaded grey gives the 11-year running averages of the open solar flux derived from the aa index, the black solid line gives the corresponding values derived from IMF observations. The dashed line is the average sunspot number, R_{11}.*

Between the start of IMF observations in 1963 and 1987, the open flux (derived from both aa and IMF observations) increased by of order 35% on average, as reported by *Lockwood et al.* [1999a; b]. The most recent data show that the downturn, seen by these authors near the end of their data sequence, has continued. This means that 1987 is now seen to be a significant peak (marked by the vertical arrow). Figure 6 also shows that the 11-year means of the sunspot number, R_{11}, has followed a similar curve. Other terrestrial data, such as the occurrence of low-latitude aurorae [*Pulkkinen et al.*, 2001], and other solar data, such as the latitudinal spread of sunspots [*Foster and Lockwood*, 2001] also show very similar variations on 10-100 year timescales.

The open magnetic flux mainly emerges through the photosphere in active regions [*Harvey and Zwann*, 1993] and is the moved around by meridional circulation, differential rotation and diffusion [*Wang et al.*, 1999a; *MacKay* et al., 2002]. *Solanki et al*. [2000, 2001] have devised a simple model of the open flux variation. This model is not concerned with how the open flux is distributed over the solar surface, rather it deals with the continuity equation of the total amount. The production (emergence) rate is quantified from a semi-empirical function of sunspot number. The loss rate is assumed to be linear, with a loss time constant that is found from the best fit to the data of *Lockwood et al*. [1999a] to be 3.6 years. In figure 7, the dashed line shows the model prediction obtained by running the model forward from an initial open flux that is taken to be zero at the end of the Maunder minimum. The model reproduces the behaviour noted by *Lockwood* [2001a] in that longer solar cycles allowed the open flux to decay away to a greater extent whereas a series of shorter cycles caused a build up in the open flux.

Note that this model was devised in 1999 to match the open flux variation in the available data, which at that time was for 1868-1996. Thus the good fit ensures that the model matches well the average open flux seen during the first perihelion pass of Ulysses, $[F_S]_{U1}$. Subsequently, the model has matched the evolution of the open flux well and therefore has correctly predicted the open flux seen by Ulysses during its second perihelion pass, $[F_S]_{U2}$ (see figure 7). Thus the model correctly reproduces the fact that the open flux near the peak of cycle 23 is only slightly larger than just before the preceding minimum, as was measured by Ulysses. This is because the cycle 23 has been a weaker cycle than its 2 predecessors (in terms of both sunspot number and open flux emergence rate), because the Ulysses pass happened to be during a relative minimum between two peaks in the solar activity, and also because the 11-year oscillation in open flux has been superposed on the downward trend that began in 1987 (see figure 6).

This modelled variation can be tested on longer timescales using records of the abundance of the cosmogenic isotopes ^{10}Be and ^{14}C found in ice sheets and tree rings, respectively. Section 3 discusses the strong anti-correlation of the open solar flux with the flux of galactic cosmic rays detected by a number of ground-based monitors. *Lockwood et al.* [2001a] has shown that there is also a significant anti-correlation between the open flux derived from aa and the abundance of the ^{10}Be isotope produced by cosmic rays (with a time lag of about one-year which is predominantly due to the time for deposition into the ice sheet). This can be seen in figure 8, in which the ^{10}Be abundance from the Dye-3 Greenland ice core [*Beer et al*., 1990; 1998] has been scaled in terms of the open flux using the best-fit linear regression (thin line). The open flux derived from the aa index is shown by the thicker solid line: this sequence has here been extended back to 1844 using data from the Helsinki magnetometer [*Nevanlinna and Kataja*, 1993]. Very good agreement can be seen between the trends in the derived open flux and in the ^{10}Be abundance, with a broad minimum around 1890, a significant rise during 1900-1960 and a subsequent fall and then rise. Thus the ^{10}Be data provide very

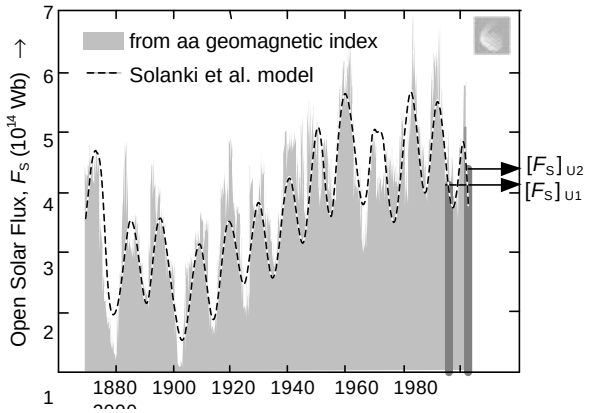

***Figure 7**. Observed and modelled variations of open solar flux. The area shaded grey gives the values derived from the aa index, as in figure 5, and the dashed line is the prediction of the model by Solanki et al. [2000]. The vertical dark grey bars give the intervals of the two perihelion passes of Ulysses, which yielded average open fluxes of $[F_s]_{U1}$ and $[F_s]_{U2}$, which are given by the horizontal arrows.*

strong support for the long-term open flux variation found from the aa index.

Figure 8 also shows, as the grey shaded curve, the open flux predicted by the model of *Solanki et al.* [2000]. However, in this case the model has been applied slightly differently. Instead of running the continuity equation forward in time from an assumed open flux of zero at the end of the Maunder minimum (as was done in figure 7), it has here been run backward in time, starting from the observed open flux at the minimum between solar cycles 22 and 23. This yields a predicted total open flux of about 1×10^{14} Wb for 1705, at the end of the Maunder minimum. This is roughly a quarter of average present- day values (figure 6). A similar

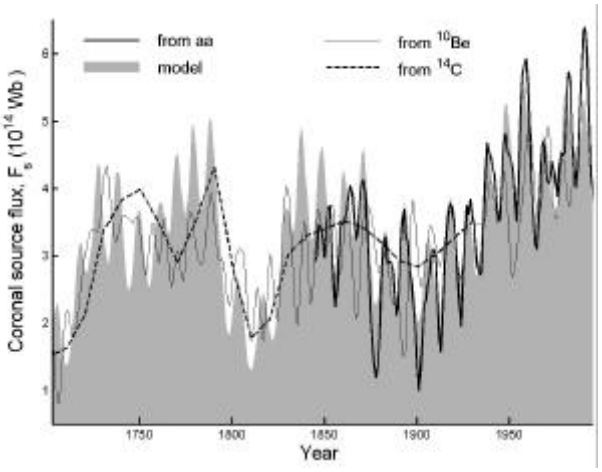

Figure 8. *Modelled, observed and inferred variations of the open flux F_s since the end of the Maunder minimum. The area shaded grey gives the predictions of the model by Solanki et al. [2000]. The thick solid line is the variation derived from the aa index, including the "Helsinki extension" data prior to 1868. The thin solid line is the abundance of the ^{10}Be isotope, as found in the Dye3 Greenland ice core and scaled as a function of F_s using a best-fit linear regression [Lockwood, 2001a]. The dashed line gives the production rate of the ^{14}C isotope, also scaled as a function of F_s using a best-fit linear regression: the production rate is determined from the isotope abundance in tree rings using a two-*

value was derived from the fit to the ^{10}Be abundances by *Lockwood* [2001a], as can be seen by the good agreement between the model and the open flux scaled from the ^{10}Be abundances in figure 8.

In addition, figure 8 shows the results of a best fit to the production rate of the ^{14}C cosmogenic isotope, deduced from a 2-reservoir model that allows for exchange between the atmosphere and the oceans and the biomass reservoirs [*Stuiver and Quay*, 1980]. The exchange with the biomass does not allow the 11-year cycles to be seen and the data after the first man-made nuclear explosions cannot be used. Nevertheless the results, shown by the dashed line, agree well with the long-term variations of the average open flux deduced from aa, from the ^{10}Be abundance and by the model. Other cosmogenic isotopes, for example, ^{44}Ti found in meteorites also indicate the long-term drift [*Bonino et al.*, 1998].

3. GALACTIC COSMIC RAYS AND THE OPEN SOLAR FLUX

The heliosphere shields the Earth from the galactic cosmic rays. The contributions of various mechanisms for deflecting cosmic rays is a matter of debate, as is the part of the heliosphere where most of the shielding takes place [e.g. *Jokipii*, 1991, *McCracken and McDonald*, 2001]. Irregularities in the field scatter the cosmic rays and the occurrence and amplitude of these irregularities, and the consequent merged diffusive barrier presented to cosmic rays, increases with the magnitude of the heliospheric field and thus with the total open solar flux. *Cane et al.* [1999] show that most of the variation of the cosmic ray fluxes is "explained" (in a statistical sense) by the strength of the heliospheric field. Only near sunspot minima the effect of polarity-dependent drifts can be seen, giving the characteristic alternate peaked and flat-topped maxima of the cosmic ray flux variation [*Ahluwalia*, 1997]. *Cane et al.* show that the tilt angle of the heliospheric current sheet is a factor near sunspot minimum and this, in turn, correlates well with the solar cycle variation in the open flux. For these reasons, the flux of cosmic rays anticorrelates strongly with the open flux. *Lockwood et al.* [2001a] found that cosmic ray fluxes observed by various neutron monitors around the globe are strongly and significantly anticorrelated with the open flux. Because the correlation coefficients c are generally between -0.8 and -0.9, the fraction of the cosmic ray variations that is statistically explained by the cosmic ray flux, c^2, is of order 0.65-0.8. The best-fit lags are generally $\Delta t < 2$ months which, for a fast,

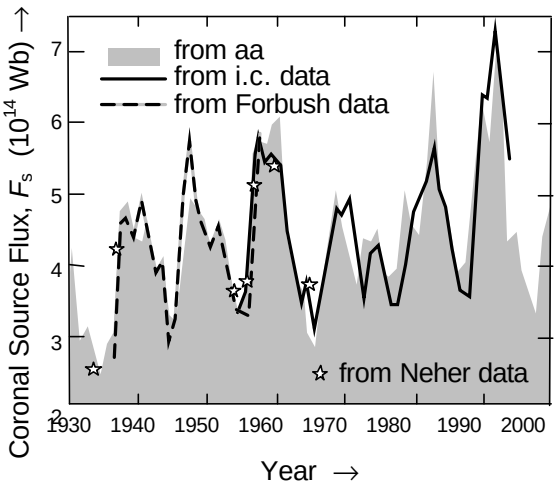

Figure 9*. Annual means of the open solar flux from the aa index (grey shaded area) compared with the variations of cosmic ray fluxes observed by a variety of ionisation chambers, scaled using linear regression fits. The solid line is the variation deduced from the data from the Fredricksberg and Yakutst instruments. The dashed line shows Forbush's original data and the stars are Neher's early data.*

polar solar wind speed of V_{sw} = 600 km s^{-1}, implies that most of the the cosmic ray shielding is at $r < \Delta t\ V_{sw} \approx$ 42 AU.

Figure 9 shows the variations from another type of cosmic ray monitor, namely ionisation chambers. The grey shaded area shows annual means of the open flux from the aa index. The solid line shows the data from the Fredricksberg and Yakutst detectors that are well intercalibrated. These data have been scaled in terms of

F_S using the best-fit linear regression. The data cover the same interval as the longer sequences of data from neutron monitors, such as Climax and the combined Huancauyo/Hawaii sequence. In this interval there is little overall drift in the open flux with a major peak in cycle 19, a weaker peak in cycle 20 followed by a return to larger values in the next two cycles. This behaviour is also seen in the scaled cosmic ray fluxes. The differences between the open flux variation and the scaled cosmic ray fluxes are smaller than the differences between the various data sequences from different cosmic ray monitors. Table 1 gives the correlations of the open solar flux from aa with the longer data sequences relevant to cosmic rays. The significance level is computed allowing for the persistence of the data, quantified by the autocorrelation of the parameters at unity lag [see *Lockwood, 2002a*, and references therein].

	Dates	c	c^2	N	r_1	D_{RMS} (10^{14} Wb)	S (%)
IMF $\|B_r\|$ & F_S	1963-2000	0.866	0.75	37	0.65	0.369	99.72
Climax n.m. C & F_S	1953-1999	-0.836	0.70	46	0.73	0.400	99.11
Hawaii n.m. H & F_S	1953-1993	-0.874	0.76	40	0.73	0.373	98.96
Ion chambers C_{ic} * & F_S	1954-1994	-0.879	0.77	40	0.71	0.365	99.52
Ion chambers C_{ic} ** & F_S	1937-1994	-0.839	0.70	57	0.68	0.375	99.93
Forbush data F & F_S	1937-1958	-0.817	0.67	21	0.35	0.340	99.81
Neher data N & F_S	1936-1958	-0.902	0.81	7	0.11	0.308	99.16

** Excludes Cheltenham data , ** Includes Cheltenham data*

Table 1. *Correlation coefficients c for correlations of annual means of various cosmic ray flux indicators with the open solar flux F_S , derived from aa: c^2 is the fraction of the variation accounted for by F_S ; N is the number of pairs of annual means; r_1 is the average ACF at lag 1; D_{RMS} is the RMS deviation from best fit; and S is the significance. The Climax and Hawaii/Huancayo neutron monitors detect rigidities greater than 3.03GV and 13.45GV respectively.*

The dashed line in figure 9 shows the results from Forbush's original data, as presented *by McCracken and McDonald* [2001]. These data were taken by a network of 5 "Carnegie Type C" ionisation chambers established in 1936-7 which were monitored closely and corrected for sensitivity changes [*Forbush*, 1958]. *McCracken and McDonald* point out that Forbush's data show a downward drift in average cosmic ray fluxes between 1936 and 1958, consistent with the downward drift in ^{10}Be isotope abundances at this time. This drift is sometimes suppressed by re-calibrations of the data which effectively assume that it is instrumental in origin: it appears as an upward drift in the average scaled open flux in figure 9, consistent with the open flux variation deduced from aa. Similarly, Neher made observations from high altitude ionisation chambers from 1933 to 1965. The intercalibration of the instruments was quoted as being better than 1% [*Neher et al.*, 1953]. Both of these early cosmic ray data sets are, like the later observations from both neutron monitors and ionisation chambers, entirely consistent with the open solar flux variation deduced from the aa index. The inferred production rate of the ^{14}C isotope provides evidence supporting the open flux variation from the aa index before 1940 and the abundances of ^{10}Be are consistent with it throughout the data sequence (figure 8). Thus the cosmic ray observations and the cosmogenic isotopes both provide strong support for the long-term variation in the open solar flux computed from the aa index, with 70-80% of the variation in cosmic ray fluxes being associated with the variation in the open solar flux. Table 1 shows that c^2 = 75% of the variation in the open flux deduced from IMF observations is explained by the variation deduced from aa. Thus some fraction of the "unexplained" variation in the cosmic ray fluxes will be due to the uncertainties of the method, including the 10% introduced by the use of the Ulysses result (see section 2.1).

4. POSSIBLE LINKS BETWEEN THE OPEN FLUX AND EARTH'S CLIMATE

In this section, we look at the correlations that must exist for either of the two possibilities implied by the paleoclimatic data discussed in the introduction. In section 4.1 we look at the correlations relevant to cosmic ray modulation of global cloud cover, using the recent extension to the cloud cover database. Section 4.2 reviews the correlations in available data between the total solar irradiance and various indicators of the open solar flux. These, like all correlations, are necessary but not sufficient in proving that a physical mechanism really exists. Because the data are global, we can be more confident that the selection effects, which have bedevilled Sun-climate correlations in the past, are not a major factor. In each case, the significance of the correlation obtained is quantified, with allowance for the persistence of the two data series: in many cases the data series are only just long enough for the correlations to be considered significant. Lastly, of course, even where a strong and statistically significant correlation between two parameters is found, this does not necessarily imply a direct causal link between them as both can be varying under the influence of other, related parameters.

4.1. Cosmic Rays and Clouds

The best correlations between cosmic rays and global cloud cover have been obtained by *Marsh and Svensmark* [2000a; b] from the infrared observations of clouds (10-12 μm) that make up the "D2" set compiled by the International Satellite Cloud Climate Project (ISCCP) [*Rossow et al.*, 1996]. This dataset is

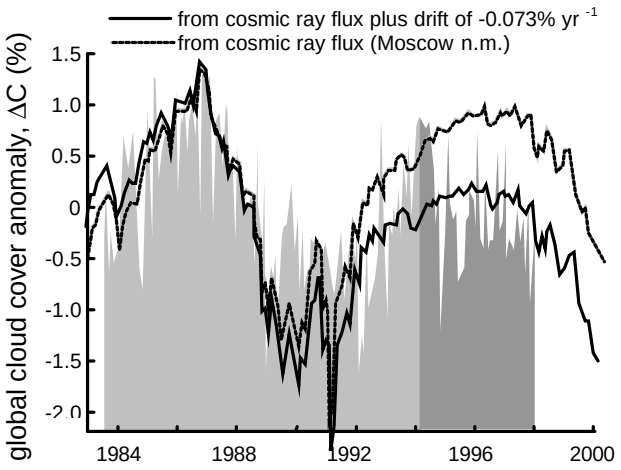

Figure 10. *The percent global cloud cover anomaly, DC for low altitude (3.2 km) cloud, seen at IR wavelengths and combined into the ISCCP D2 dataset. The light grey shaded area shows the original dataset for which Marsh and Svensmark [2000] discovered the solar cycle variation, with a strong correlation with cosmic ray fluxes. The darker grey area is the variation of the recently-added data for after 1994. The dotted line shows the cosmic ray counts (scaled from the best-fit linear regression) from the Moscow neutron monitor. The solid line shows the best-fit combination of the cosmic ray flux variation added to a downward linear drift at a rate of 0.073% yr*$^{-1}$.

compiled from observations from a wide variety of spacecraft and inter-calibration of the instruments is problematic. The correlation is not found for all clouds, in fact it is only present for cloud-top pressures exceeding 680 hPa, and thus corresponds to altitudes below about 3.2 km.

Figure 10 illustrates this correlation in monthly means of the data, de-trended to remove annual variations. The light grey area shows the full cloud clover anomaly (ΔC) dataset that was available until late last year (covering the interval 1983-1994) and the dotted line shows the cosmic ray flux from the Moscow neutron monitor (which detects the products of cosmic rays of rigidity 2.46GV and above: the results for other stations are very similar). The peak correlation coefficient is c = 0.65, with a best-fit lag of 4 months introduced into the cloud cover data sequence. This means that c^2 = 42% of the variation in the cloud cover could be attributed to the cosmic rays. The significance of the correlation, S is very high at 99.3% (i.e. there is only a 0.7% probability that this result was obtained by chance). If we introduce smoothing into the time series the correlation coefficient is greatly increased, rising to c = 0.914 for 12-month running means (c^2 = 84%). However, this increases the persistence in the data series and the result can no longer be considered statistically significant. In order to achieve a significance of 99%, a correlation of this level would need to be maintained in smoothed data from a further 50 years. Some authors [e.g. *Kristjánsso and Kristiansen*, 2000] have questioned the validity of this correlation but *Marsh and Svensmark* have used other means to check its validity by producing global spatial maps of the correlation and looking at its coherence. They find that it is primarily liquid, maritime clouds, away from regions of an El-Niño event, that correlate well. A similar conclusion has been reached by *Udelhofen and Cess* [2001] in ground-based data from 90 weather stations across the North American Continent. Instrument relocation and changes mean that a long-term drift in these ground-based data cannot be determined, but de-trended data show a clear and persistent solar cycle variation in coastal cloud cover, of the type shown in figure 10, in data that extends back to 1900. Recent ground-based studies by *Goode et al.* [2001] of the "Ashen light", the Earthshine reflected back by the dark side of the moon, also show a the variation consistent with that reported by *Marsh and Svensmark*.

Recently, the D2 dataset has been extended to cover period after 1994. The new data, shown in dark grey in figure 10, appear to show the correlation breaking down. *Marsh and Svensmark* [2002] have pointed out that there may be problems in the intercalibration between the old and the new data. The evidence for this is that there is a simultaneous sudden jump in the overlying cloud cover at greater altitudes in the combined data, and that some datasets do not show such a major and sudden decrease during 1994 as in these D2 data. In particular, these authors have made a comparison with independent observations of clouds obtained from the SSMI instrument onboard the DMSP satellites. This instrument operates at microwave wavelengths, which are able to penetrate ice and dust clouds, and thus observe liquid water clouds. This cloud data is available over the oceans for periods between July 1987 - June 1990 and Jan 1992 - Oct 2001. The 18 month gap is due to a problem with one of the sensor's 4 channels; however, on board calibration was maintained during this period using the 3 remaining channels. Since it is liquid clouds that give the correlation in the D2 data, this is a good data set with which to check this part of the ISCCP low cloud dataset. Differences and drifts between the two datasets do exist and it is possible that the growing discrepancy between the new D2 data and the cosmic ray flux variation is caused by an instrumental effect.

However, there is another possibility – namely that the drift is real and is caused by an independent effect that works in concert with the proposed cosmic ray modulation. Figure 11 shows the results of global simulations of the coupled ocean-atmosphere system by Stott and co-workers at the Hadley Centre for Climate Change. The predictions are made by the HAD3CM ocean-atmosphere global circulation model. The bottom panel [from *Stott et al.*, 2000] compares the observed global warming curve (dashed line), with the predicted global average temperature anomaly ΔT, derived from the model using best fits to the global spatial patterns of temperature change (grey shaded area).

Model inputs allow for the variability of all climate forcings, including solar irradiance [from *Lean et al*., 1995], volcanic activity, sulphate pollution and anthropogenic greenhouse gasses. The simulation shown here is one of an ensemble produced by *Stott et al.* [2000] and gives the red curve in Figure 1 of their paper. The upper panel of figure 11 shows the percent low-altitude cloud cover anomaly ΔC predicted by the same simulation run.

The interesting point is that the predicted global cloud cover is relatively constant before 1975, declining at an average of only 0.01% yr^{-1} between 1910 and 1975. However, after 1975 the cloud cover declines much more rapidly, at an average of 0.079% yr^{-1}. This more rapid decline appears to be associated with the dominant anthropogenic warming in the average temperature simulation for these years. Based on this, it is interesting to speculate that the drift in the D2 data may in fact be real. The solid line in figure 10 shows the best-fit multi-variable fit to the D2 low-altitude data, using the Moscow cosmic ray counts and an independent linear variation. The best fit is obtained with a decline in cloud cover at 0.073% yr^{-1} over the interval 1982-1998 – very similar to the drift predicted by the global simulation. With the addition of this linear decline, the correlation found by Svensmark is improved slightly, but the significance remains roughly the same because

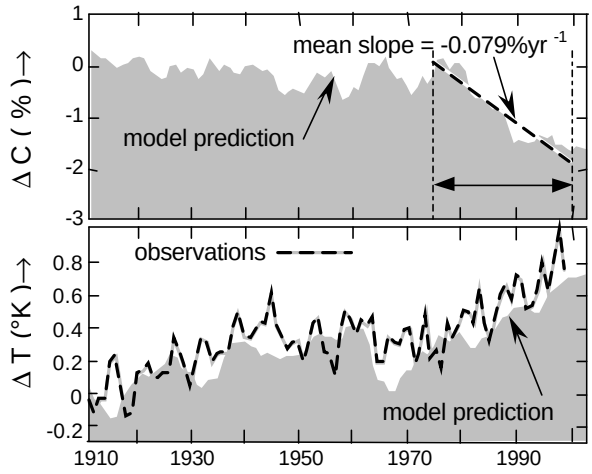

Figure 11. *Model predictions made by the Hadley Centre's HAD3CM ocean-atmosphere global circulation model. The bottom panel (from Stott et al., 2000) compares the observed global warming curve (dashed line) with the predicted global average temperature anomaly DT, derived from the model using best fits to the global spatial patterns of temperature change (grey shaded area). Model inputs allow for the variability of various climate forcings, including solar irradiance (Lean et al., 1995), volcanic activity, sulphate pollution and anthropogenic greenhouse gasses. The upper panel shows the percent low-altitude cloud cover anomaly DC predicted by this simulation. (Courtesy of Peter Stott, UK Meteorological Office).*

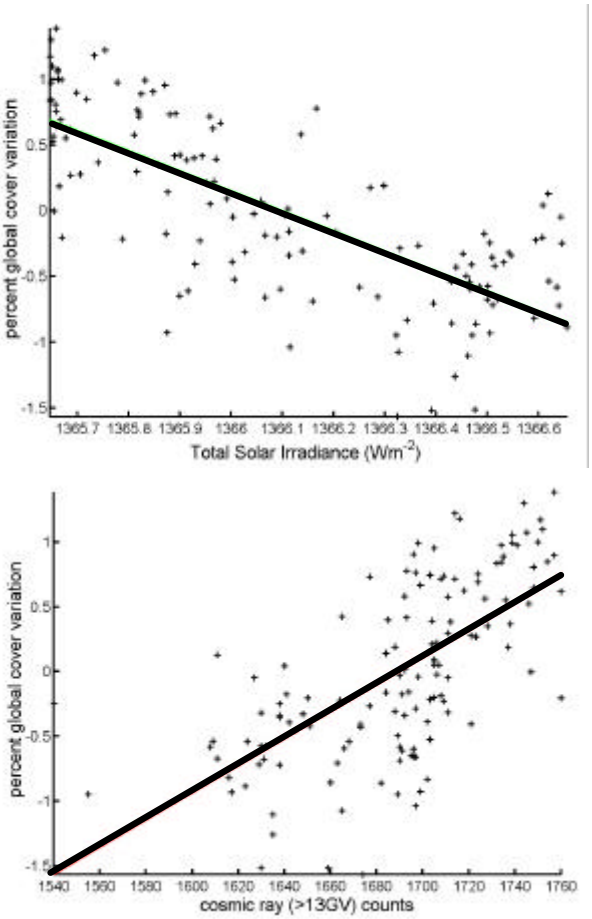

Figure 12. *Scatter plots of low-altitude cloud cover anomaly, DC (from the ISCCP D2 dataset) as a function of (top) the total solar irradiance, TSI and (bottom) the cosmic ray counts recorded at Huancauyo/Hawaii (rigidity cut off 13 GV). The solid lines give the best-fit linear regressions [from Lockwood,*

the effects of the increased correlation and of the longer data sequence are offset by the increased number of degrees of freedom. This can be considered, at best, as only an indication of a possibility because the model does not contain any mechanisms for ion-induced cloud nucleii condensation and it is quite likely that if such a mechanism did exist, it would not be independent of the anthropogenic effect on cloud cover suggested by figure 11.

The data shown in Figure 10 and the studies by *Marsh and Svensmark* [2000a; b] and *Udelhofen and Cess* [2000] do appear to show that there is a solar cycle variation in cloud cover. However, we must be cautious in ascribing this variation purely to the direct effect of cosmic rays. Figure 12 shows scatter plots of monthly data relating the observed cloud cover anomaly (seen in the D2 dataset up to 1994) to, in the bottom panel, the cosmic ray flux (this time seen at Hauancayo/Hawaii for which rigidity exceeds 13 GV) and, in the top panel, the total solar irradiance (TSI). The TSI data are version 21 of the composite total solar irradiance dataset prepared and provided by PMOD/WRC, Davos. Ver-

sions 3 and 8 of this dataset are described by *Fröhlich and Lean*, [1998a] and [1998b], respectively. The main instruments used were HF on the Nimbus 7 satellite, ACRIM 1 on SMM, ERBS, ACRIM 2 on UARS and the VIRGO instrument on SoHO. Other data considered are from JPL rocket flights and PMOD rocket and balloon flights, and from the SOVA2 instrument. The main changes made since version 8 are: the ACRIM II slip around 3 October 1995 was removed by adding 0.12 Wm^{-2} after that date; the VIRGO data were updated to the end of May, 2001; the ACRIM II data updated and a new version from R.C Willson incorporated; the NIMBUS correction was improved and an improved algorithm for calculation of VIRGO data was introduced [*Fröhlich*, 2000].

The peak correlation coefficients for the data shown in figure 12 were -0.741 and +0.654 (for TSI - cloud cover and cosmic ray flux - cloud cover, respectively). These correlations are significant at the 99.8% and 99.6% levels. Although the correlation is marginally higher for TSI than for the cosmic rays, application of the Fisher-Z test [*Lockwood, 2002a*] shows that the difference between these two correlations is not significant (the significance level of the difference being only 30% so the probability that the difference arose by chance is 0.7).

Therefore, although the presence of a strong and persistent solar cycle variation in cloud cover implies a solar/heliospheric effect, from these correlations we cannot tell which of the two mechanisms implied by the paleoclimate studies is at work (or what combination of the two). The data are sufficient to confirm that a mechanism whereby cosmic rays modulate the production of clouds could be effective, but alternatively, the cloud cover variation may be, at least in part, a terrestrial response to the solar cycle variation in the total solar irradiance.

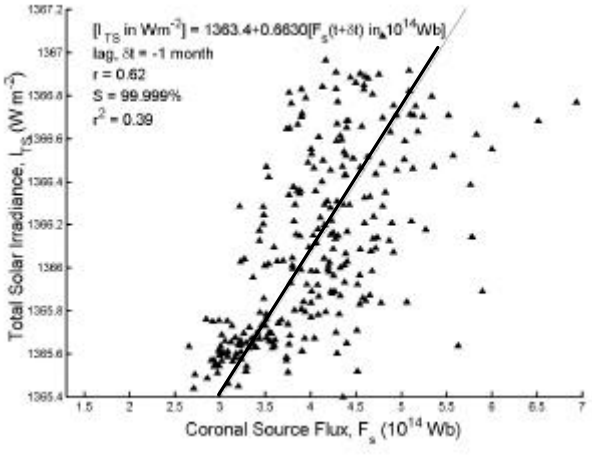

Figure 13. *Scatter plot of the open solar flux (derived from IMF observations) and the total solar irradiance, I_{TS}. The solid line gives the best-fit linear regression. The I_{TS} data are the composite date series compiled by Fröhlich[2000]. [from Lockwood,*

4.2. Open Flux and Irradiance

The correlations shown in figure 12 imply that there must be a strong correlation between the open solar flux and the total solar irradiance (and thus, from section 3, an anticorrelation between the irradiance and the cosmic ray flux). Such correlations have been reported by *Lockwood and Stamper* [1999] and *Lockwood* [2002a].

Figure 13 presents the scatter plot and best-fit linear regression between the open solar flux, derived from IMF measurements using equation (1), and the TSI from the composite dataset used in the last section. The data are monthly means and the peak correlation of c = 0.62 (c^2 = 0.39) is found at a lag of 1 month. The significance of this correlation, allowing for persistence, is 99.999%

	Dates	c	c^2	N	r_1	S (%)	L* (mon)
$\langle F_S \rangle$ & $\langle I_{TS} \rangle$	Jun 1979 – Nov 2000	0.800	0.641	272	0.994	-	6
F_S & I_{TS}	Oct 1978 – Mar 2001	0.621	0.385	270	0.748	99.999	14
$\lvert B_r \rvert$ & I_{TS}	Oct 1978 – Mar 2001	0.489	0.240	255	0.725	99.94	-1
Moscow M & I_{TS}	Oct 1979 – Nov 2000	-0.713	0.508	262	0.966	90.3	3
Climax C & I_{TS}	Oct 1979 – Nov 2000	-0.716	0.513	262	0.970	85.5	3
Hermanus H_e & I_{TS}	Oct 1979 – Nov 1999	-0.736	0.542	239	0.961	91.6	3
Tblisi T_b & I_{TS}	Oct 1979 – Sep 1997	-0.805	0.649	230	0.939	95.8	2
Tsumeb T_s & I_{TS}	Oct 1979 – Jan 1999	-0.785	0.617	230	0.939	98.3	3
Hawaii H & I_{TS}	Oct 1979 – Oct 2000	-0.832	0.692	252	0.971	90.3	-1
$\langle M \rangle$ & $\langle I_{TS} \rangle$	Mar 1982 – May 2000	-0.929	0.863	219	0.997	-	4

(I_{TS} leading)*

Table 2. *Correlation coefficients c for correlations of monthly means of various cosmic ray flux and open solar flux indicators with the total solar irradiance, I_{TS} : c^2 is the fraction of the variation in I_{TS} explained ; N is the number of pairs of monthly means; r_1 is the average ACF at lag 1; S is the significance; and L is the best fit lag (with I_{TS} leading). The geomagnetic cut-off rigidities for the various neutron monitors are: Moscow, 2.46GV; Climax, 3.03GV; Hermanus, 4.9GV; Tblisi, 6.91GV; Tsumeb, 9.29GV; Hawaii-Huancayo, 13.45GV. The first and last rows are for 12-point running means of the monthly data.*

Table 2 summarises other correlations between the total solar irradiance I_{TS} and the open solar flux F_S or cosmic ray fluxes. The correlations are all significant for monthly data. Smoothing the data increases the correlation coefficient but usually removes its significance. The anticorrelations between TSI and the various cosmic ray fluxes are strong (typically –0.7 to –0.85) and significant (S = 90-98%).

Thus we can say that TSI and cosmic ray fluxes are anti-correlated over recent solar cycles. This may mean no more, physically, than the fact that both the irradiance and heliospheric shield go up and down with the solar activity cycle. The real question is "will such a correlation hold on 100 to 1000 year timescales?". Were this to be true, it would certainly imply that there is a substantive physical reason why the open flux is a good proxy for TSI. At present, there are only two reasons to suspect that this might be the case. The first is supplied by the paleoclimate studies showing relationships between terrestrial climate and cosmogenic isotopes, as discussed in section 1.1. The second is the considerable similarity between the extrapolation of TSI using the open flux and independent reconstructions of the variation of TSI, as discussed in the next section.

4.3 Reconstructions of the Past Variation in the Total Solar Irradiance

The discovery that the total solar irradiance (TSI) has varied with sunspot number over recent sunspot cycles [*Willson*, 1997; *Fröhlich and Lean*, 1998a; b; *Fröhlich*, 2000] leads to the important question of how it has varied on the 100-year timescales of the Gleissberg cycle and on the 1000-year timescales of the cosmogenic isotope fluctuations during the holocene. For studies of modern terrestrial global warming, the recent 100-year variations are of particular importance: we know how sunspot number varied over this period but have to reconstruct the TSI variation using proxies.

A number of proxies have been used. *Hoyt and Schatten* [1993] used a combination of the sunspot number and the length of the sunspot cycle. The main justification for deriving the long-term drift from the solar cycle length comes from the connection between solar cycle length and global mean surface temperature on Earth reported by *Friis-Christensen and Lassen* [1991]. Thus use of this reconstruction for studies of the effect of TSI changes on climate are problematical and leads to circular arguments.

The TSI reconstructions by *Lean et al.* [1995], *Lean* [2000] and *Solanki and Fligge* [1998; 1999] used a combination of sunspot number, R, with the 11-year running means of the sunspot number, $\langle R \rangle_{11}$. The rationale for the use of this combination lies, to some extent, with our understanding of the origin of recent TSI variations. Sunspots are larger, cooler flux tubes (radius greater than about 250 km) which lower the TSI because the upward heat flux to the photospheric surface is blocked [*Spruit*, 1991], yet at recent sunspot maxima the TSI has peaked. This is ascribed to the larger nett effect of the smaller, facular flux tubes. These maintain their temperature by radiation from the surrounding "walls" but the reduced particle concentration (to compensate the enhanced magnetic pressure) means that the r of constant optical depth is lowered in the faculae and we receive radiation from deeper, hotter layers [*Lean*, 1991]. Models accounting for the total TSI variation in terms of these surface magnetic effects, use indices of faculae to quantify their brightening effect have been successful in reproducing variations in TSI on timescales of days up to the solar cycle [*Fligge*, 1998; *Fröhlich and Lean*, 1998a].

The Sun is almost devoid of spots at each minimum (although, in fact, inspection of the record shows that the sunspot number at minimum did rise slightly during the last century, with a waveform rather similar to that seen in both $\langle R \rangle_{11}$ and F_S (as given in figure 6). Thus use of just R as a proxy would mean that TSI always returned to roughly the same minimum value and there could be no long-term drifts in TSI which could accrue from a long-term change in the number, size and/or contrast of faculae. Use of $\langle R \rangle_{11}$ allows such a drift but assumes that is shares a common long-term variation waveform. *Lean et al.* [1995] and *Lean* [2000] quantify the amplitude of this drift by comparing the Sun at the Maunder minimum with the brightness of non-cyclic Sun-like stars.

The surprising fact is that these reconstructions are very similar in form and amplitude to the simple extrapolation of TSI by *Lockwood and Stamper* [1999], based on the high correlation and a simple linear regression with the open solar flux, F_S. *Lockwood* [2001a] has pointed out that it is not so surprising that these reconstructions in TSI are all similar in form. This is because the various proxies used to define the long-term drift (namely solar cycle length, $\langle R \rangle_{11}$ and $\langle F_S \rangle_{11}$) are all highly correlated. What is surprising, however, is the great similarity between the amplitudes of the long-term drifts – in particular for the reconstruction by *Lean* [2000] and extrapolation by *Lockwood and Stamper* [1999]. Essentially, is the reconstruction of *Lean* [2000] is correct, then the open solar flux must be an excellent proxy for TSI, on century timescales as well as on decadal timescales.

5. DISCUSSION AND IMPLICATIONS

In this paper we have looked at correlations and possible links between open solar flux, total solar irradiance, cosmic ray fluxes and terrestrial cloud cover and climate. Over recent solar cycles, each has varied with the other, making untangling the potential mechanism(s) for influencing Earth's climate very difficult. Without a physical understanding of these correlations, we cannot extrapolate back to earlier times and so evaluate the effect that they may have had, nor can we evaluate recent reports of direct correlations between atmospheric parameters and coronal hole area and open flux [e.g. *Soon et al.*, 2000]. Several important climate parameters are showing apparent solar cycle variations (in addition to the cloud cover data discussed in section 4.1) - often in good agreement with the TSI record. For example *White et al.* [1997; 1998] find sea surface temperature variations for all the Earth's major oceans on 11-year timescales. The large thermal capacity of the oceans means that these fluctuations are not detected in global surface temperatures [*Wigley and*

Raper, 1990; *Cubasch et al.*, 1997]; however, caution is needed because ocean oscillations can have beat periods on these timescales.

Figure 14 investigates the possible role of solar variability on 100-year timescales on global climate change. A fuller, updated description of this work is given by *Stott et al*. [2000], here use a simpler prediction by *Hill et al.* [2000] to illustrate the principles. The Hadley Centre's HAD3CM general circulation model was used, with inputs representing volcanic, solar (the *Lean et al.* [1995] TSI reconstruction was used), and anthropogenic forcings. Fits were made to the observed global spatial pattern to the predicted temperature anomaly response [*Tett et al*., 1999]. Figure 14 shows that a very good match to the sampled global warming curve was achieved. The figure also shows the variations of natural and man-made effects on the temperature and the causes of change in various sectors of these graphs are labelled. Of particular note is that the solar effect was mainly in the interval 1907-1947 whereas the anthropogenic contribution was dominant after 1967. Thus the solar and anthropogenic forcing increases were at different times and amplifying one will not necessarily decrease the other. In order to get the fit shown in the figure, amplification factors were required, relative to the predictions from radiative forcing [*Hansen et al*., 1997]. The best fit required that the solar effect be amplified by a factor 2.5. This increased solar influence allowed a much better fit to the peak in the temperature curve around 1947. The work of *Stott et al*. [2000] finds an even larger factor of 3. At the 90% confidence level this solar amplification is between 1 and 6. Interestingly, the best fit also required an amplification of the anthropogenic greenhouse effect (by a more modest factor of 1.15). Thus enhanced solar contribution appears to imply an enhanced sensitivity to anthropogenic effects, but with the onset of the latter somewhat later.

These global climate simulations call for a mechanism which amplifies the solar effect above what one would expect from radiative forcing by the reconstructed TSI variation. A number of possibilities have been proposed. The cosmic ray – cloud mechanism discussed in section 4.1 would certainly be one. Another is that spectral irradiance changes in the UV have a disproportionate effect [*Haig*, 1994; 1999a; b; 2001; *Shindell et al*., 1999; 2001; *Larkin et al*., 2000]. These are known to cause solar cycle variations in the stratosphere, where they modulate the quasi-biennial oscillation [*Labitzke and van Loon*, 1997; *Gray et al*., 2001] and it has been proposed that these may propagate down into the troposphere. Other possibilities may involve the modulation of the global electric circuit [*Bering et al.*, 1998] by air ions produced by comic rays [*Markson*, 1981; *Harrison*, 2002a]: recent results show mid-latitude thunderstorm activity is modulated by the solar cycle [*Schlegel et al.*, 2001] and there is evidence for a century-scale drift in the global electric current [*Harrison*, 2002b].

Whatever the cause, evidence is growing that the solar influence on climate over the past 150 years is somehow amplified. From the point of view of solar and heliospheric physics, this raises some very interesting questions about the relationship of solar irradiance, open flux and cosmic rays. It is surprising that the open flux appears to be related to TSI because TSI is modulated by the photospheric field and will depend on the total field and the distribution of flux tube sizes (or, more crudely, the ratio of the total areas covered by sunspots to faculae). The open flux, on the other hand, is a small fraction of the total photospheric flux [*Wang et al*., 1999b]. The origins of an understanding may be inherent in the modelling of *Solanki et al.* [2002] who find that the open flux is an almost constant fraction of the total photospheric flux. Only once these potential connections are understood will be able to answer why cosmogenic isotopes and Earth's climate appear to be so well linked on a range of timescales and to use them as indicators of solar influence on climate with greater confidence.

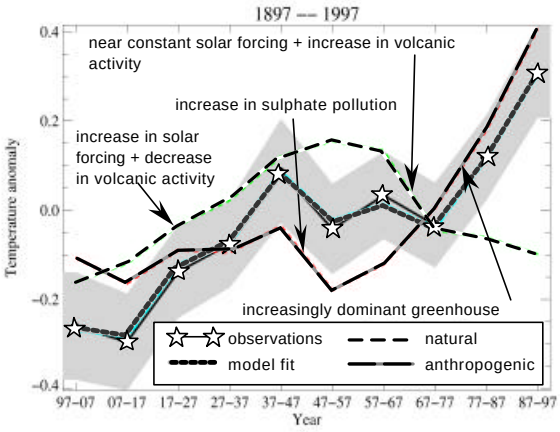

Figure 14. *Analysis of the contributions to a model fit to the global warming curve. The fits to the sampled temperature record were made on the spatial patterns of temperature change, using the HAD3CM model. The contributions of natural and man-made forcings are shown separately and some of the dominant effects on the variations are labelled. To obtain this fit, the solar forcing was amplified by a factor 2.5, relative to the predicted radiative forcing caused by solar irradiance change reconstruction by Lean et al [1995]. The anthropogenic forcing was amplified by a factor 1.15. From Hill and Allen*

Acknowledgments: The author is grateful for discussions with, and preprints from, a number of scientists concerning their recent work; in particular, S. Solanki, N. Marsh, H. Svensmark, Y.-M. Wang, J. Kirkby, M. Allen, J. Haig, K. McCracken, T.D.G. Clark and J. Lean. He is also grateful to J. Beer, who supplied the ^{10}Be isotope data from the Dye3 Greenland ice core, to C. Fröhlich and PMOD, Davos for the total solar irradiance composite dataset, to A. Balogh and the team at Imperial College, London who supplied the Ulysses

magnetometer data, to D. McComas who supplied the Ulysses solar wind data and to the World Data Center system for collecting, archiving, and distributing the cosmic ray data. He thanks P Stott of the UK Meterological Office for the global cloud cover simulations. This work was supported by the U.K. Particle Physics and Astronomy Research Council.

REFERENCES

Ahluwalia, H.S., Galactic cosmic ray intensity variations at a high-latitude sea-level site 1937-1994, *J. Geophys. Res., 102*, 24,229-24,236, 1997

Balogh, A., et al., , The heliospheric field over the south polar region of the Sun, *Science, 268*, 1007-1010, 1995.

Bard, E., et al., Solar modulation of cosmogenic nuclide production over the last millenium: comparison between ^{14}C and ^{10}Be records, *Earth and Planet. Sci. Lett., 150*, 453-462, 1997.

Beer, J., Long-term indirect indices of solar variability, *Space Sci. Rev., 94 (1/2)*, 53-66, 2000.

Beer, J., et al., Use of ^{10}Be in polar ice to trace the 11-year cycle of solar activity, *Nature, 347*, 164-166, 1990.

Beer, J., S. Tobias, and N. Weiss, An active Sun throughout the Maunder minimum, *Sol. Phys., 181*, 237-249, 1998.

Bering, E.A., A.A. Few, and J.R. Benbrook, The global electric circuit, *Phys. Today, 51*, 24-30, 1998.

Bond, G., et al., Persistent solar influence on North Atlantic climate during the Holocene, *Science, 294*, 2130-2136, 2001.

Bonino, G., G. Cini Castognoli, N. Bhabdari and C, Taricco, Behavior of the heliosphere over prolonged solar quiet periods by ^{44}Ti measurements in meteorites, *Science, 270*, 1648-1650, 1998.

Cane, H.V., G. Wibberenz, I.G. Richardson, and T.T. von Rosenvinge, Cosmic ray modulation and the solar magnetic field, *Geophys. Res. Lett., 26*, 565-568, 1999.

Clilverd, M.A., T.D.G. Clark, E. Clarke, and H. Rishbeth, Increased magnetic storm activity from 1868 to 1995, *J. Atmos. Sol.-Terr. Phys., 60*, 1047-1056, 1998.

Cliver, E.W., V. Boriakoff, and K.H. Bounar, The 22-year cycle of geomagnetic activity, *J. Geophys. Res., 101*, 27,091-27,109, 1996.

Couzens, D. A. and J. H. King, Interplanetary Medium Data Book - Supplement 3, National Space Science Data Center, Goddard Space Flight Center, Greenbelt, Maryland, USA, 1986.

Cubasch, U., et al., Simulation of the influence of solar radiation variations on the global climate with an ocean-atmosphere general circulation model. *Clim. Dyn., 13*,.757-767, 1997.

Finch, I., M. Lockwood and R.Stamper, Solar wind-magnetosphere coupling functions on timescales of 1day to 1 year, *Annales Geophys*., submitted, 2002.

Fligge, M., et al., A model of solar total and spectral irradiance variations, *Astron. Astrophys*., *335*, 709-718, 1998.

Forbush, S.E., Cosmic ray intensity variations during two solar cycles, *Geophys. Res*., 63, 651-669, 1958.

Foster, S., and M. Lockwood , Long-Term Changes in the Solar Photosphere Associated with Changes in the Coronal Source Flux, *Geophys. Res. Lett., 28*, 1443-1446, 2001.

Friis-Christensen, E., and K. Lassen, The length of the solar cycle, an indicator of solar activity closely associated with climate, *Science, 192*, 1189-1202, 1991.

Fröhlich, C. and J. Lean, Total Solar Irradiance Variations, in New Eyes to see inside the Sun and Stars, ed. F.L. Deubner et al., eds. Proceedings IAU Symposium 185, Kyoto, August 1997, Kluwer Academic Publ., Dordrecht, The Netherlands, pp. 89-102 1998a

Fröhlich, C., and J. Lean, The Sun's total irradiance: Cycles, trends and related climate change uncertainties since 1976, *Geophys. Res. Lett., 25*, 4377-4380, 1998

Fröhlich, C., Observations of Irradiance Variations, *Space Sci. Rev., 94 (1/2)*, 15-24, 2000.

Gazis, P.R., Solar cycle variation of the heliosphere, *Rev. Geophys., 34*, 379-402, 1996.

Gleissberg, W., A table of secular variations of the solar cycle, *J. Geophys. Res., 49*, 243-244, 1944.

Goode, P.R., et al., Earthshine observations of the Earth's reflectance, *Geophys. Res. Lett., 28*, 1671-1674, 2001

Gray, L.J., et al., A data study of the influence of the equatorial upper stratosphere on northern hemisphere stratospheric sudden warmings, *Q.J.R. Meteorol. Soc., 127*, 1985-2003, 2001.

Haigh, J. D. , The role of stratospheric ozone in modulating the solar radiative forcing of climate. *Nature, 370*, 544-546, 1994

Haigh, J. D., A GCM study of climate change in response to the 11-year solar cycle. *Quart. J. Roy. Meteorol. Soc., 125*, pp.871-892, 1999a

Haigh, J. D., Modelling the impact of solar variability on climate. *J. Atmos. Solar-Terrest. Phys., 61*, 63-72, 1999b

Haig, J.D., Climate variability and the influence of the Sun, *Science, 294*, 2109-2111, 2001.

Hansen, J., M. Sato, and R. Ruedy, Radiative forcing and climate response, *J. Geophys. Res., 102*, 6831-6864, 1997.

Hapgood, M.A., A double solar-cycle variation in the 27-day recurrence of geomagnetic activity, *Ann. Geophys., 11*, 248-256, 1993.

Harrison, R. G. and K.L. Alpin, Atmospheric condensation nuclei formation and high-energy radiation, *J. atmos. Terr. Phys., 63*, 1811-1819, 2001.

Harrison, R.G., Radiolytic particle production in the atmosphere *Atmos Environ* 36, 169-160, 2002a

Harrison, R.G., Secular decrease in the global atmospheric electric circuit from cosmic rays, *Science*, submitted, 2002b

Harvey, K.L., and C. Zwaan, Properties and emergence of bipolar active regions, *Sol. Phys.*, 148, 85-118, 1993.

Hill, D., et al., Natural and anthropogenic causes of recent climate change. RAL Internal Report, 2000.

Hoyt, D., and K. Schatten, A discussion of plausible solar irradiance variations 1700-1992, *J. Geophys. Res., 98*, 18,895-18,906, 1993.

Kirkby, J., CLOUD: A particle beam facility to invetsigate the influence of cosmic rays on clouds, *Proc. Workshop on Ion-Aerosol-Cloud Interactions, CERN, 18-20th April 2001*, ed. J. Kirkby, CERN Yellow Report, CERN-2001-007 (ISSN 0007-8328, ISBN 92-9083-191-0), 2001.

Jokipii, J.R., Variations of the cosmic ray flux with time, *in "The Sun in Time"*, eds. C.P. Sonnet, M.S. Giampapa and M.S. Matthews, Univ. of Arizona Press, pp. 205-221 ISBN 0-8165-1297-3, 1991

Kristjánsson, J.E., and J. Kristiansen, Is there a cosmic ray signal in recent variations in global cloudiness and cloud radiative forcing?, *J. Geophys. Res., 105*, 11,851-11,863, 2000.

Labitzke, K. and van Loon, H., The signal of the 11-year sunspot cycle in the upper troposphere-lower stratosphere. *Space Sci. Rev., 80*, 393-410, 1997

Larkin, A., J. D. Haigh, S. Djavidnia, The Effect of Solar UV Irradiance Variations on the Earth's Atmosphere, *Space Sci. Rev., 94(1/2)*, 199-214, 2000.

Lean, J., Variations in the Sun's radiative output, *Rev. Geophys, 29(4)*, 505-535, 1991

Lean, J., Evolution of the Sun's spectral irradiance since the Maunder minimum, *Geophys. Res. Lett., 27 , 2425-2428*, 2000.

Lean, J., J. Beer, and R. Bradley, Reconstruction of solar irradiance since 1610: Implications for climate change, *Geophys. Res. Lett., 22*, 3195-3198, 1995.

Lockwood, M., Long-Term Variations in the Magnetic Fields of the Sun and the Heliosphere: their origin, effects and implications, *J. Geophys. Res., 106*, 16021-16038, 2001a.

Lockwood, M., Long-term variations in cosmic ray fluxes and total solar irradiance and global climate change, *Proc. Workshop on Ion-Aerosol-Cloud Interactions, CERN, 18-20th April 2001*, ed. J. Kirkby, CERN Yellow Report, CERN-2001-007 (ISSN 0007-8328, ISBN 92-9083-191-0), 2001b.

Lockwood, M., An evaluation of the correlation between open solar flux and total solar irradiance, *Astron and Astrophys.*, 382, 678-687, 2002a

Lockwood, M., The relationship between the near-Earth interplanetary field and the coronal source flux: dependence on timescale, *J. geophys. Res.*, submitted, 2002b.

Lockwood, M., Long-term variations in cosmic ray fluxes and total solar irradiance and their possible influence on global climate change, *J. atmos. Terr. Phys.*, submitted, 2002c

Lockwood, M., and S.S. Foster, Long-term variations in the magnetic field of the Sun and possible implications for terrestrial climate, *in "The solar cycle and Terrestrial Climate"*, Proc. 1st. Solar and Space Weather Euroconference, ESP SP-463, 85-94, 2001.

Lockwood, M., and R. Stamper, Long-term drift of the coronal source magnetic flux and the total solar irradiance, *Geophys Res. Lett., 26*, 2461-2464, 1999.

Lockwood, M., R. Stamper, and M.N. Wild, A doubling of the sun's coronal magnetic field during the last 100 years, *Nature*, 399, 437-439, 1999a.

Lockwood, M., et al., Our changing Sun, *Astron. Geophys, 40*, 4.10-4.16, 1999b.

Lockwood, M., R.B. Forsyth, A. Balogh, and D. J. McComas, The accuracy of open solar flux estimates from near-Earth measurements of the interplanetary magnetic field: analysis of the first two perihelion passes of the Ulysses spacecraft., *.J geophys. Res.*, to be submitted, 2002.

Markson R., Modulation of the Earth's electric field by cosmic radiation, *Nature 291*, 304-308, 1981

Marsh N. and H. Svensmark, Low Cloud Properties influenced by Cosmic Rays, *Physical Review Letters, 85*, 5004-5007, 2000a.

Marsh, N., and Svensmark, H., Cosmic rays, clouds and climate, *Space Sci. Rev., 94 (1/2)*, 215-230, 2000b

Marsh N. and H. Svensmark, GCR and ENSO trends in ISCCP-D2 low cloud properties, *J. geophys. Res.*, submitted, 2002

Mayaud, P.N., The *aa* indices: A 100-year series characterising the magnetic activity, *J. Geophys. Res., 77*, 6870-6874, 1972.

McCracken, K.G., and F.B. McDonald, The long-term modulation of the galactic cosmic radiation,

1500-2000, in press, *in Proc. 27th. Int. Cosmic Ray Conference*, Hamburg, 2001

Mackay, D. H., E. R. Priest, and M. Lockwood, The Evolution of the Sun's Open Magnetic Flux: I. A Single Bipole,. *Solar Physics*, in press, 2002

Neher, H.V., V.Z. Peterson, and E.A. Stern, Fluctuations and latitude effect of cosmic rays at high altitudes and latitudes. *Phys. Rev., 90*, 655-674, 1953.

Nevanlinna, H. and E. Kataja, An extension to the geomagnetic activity index series aa for two solar cycles (1844-1868), *Geophys. Res. Lett., 20*, 2703-2706, 1993.

O'Brien, K., Secular variations in the production of cosmogenic isotopes in the Earth's atmosphere, *J. Geophys. Res., 84*, 423-431, 1979.

Pulkkinen, T.I., H. Nevanlinna, P.J. Pulkkinen, and M. Lockwood, The Earth-Sun connection in time scales from years to decades to centuries, *Space Sci. Rev., Space Sci. Rev., 95(1/2)*, 625-637, 2001.

Rast, M. P., et al., Bright rings around sunspots, *Nature, 401*, 678 – 679, 1999

Rossow, W.B., A.W. Walker, D.E. Beuschel, and M.D. Roiter, International Satellite Cloud Climatology Project (ISCCP): Documentation of new datasets, WMO/TD 737, World Meteorol. Organ., Geneva, 1996.

Schatten, K.H., Models for Coronal and Interplanetary magnetic fields: a critical commentary, in "Sun-Earth plasma connections", ed. J.L. Burch, R.L. Carovillano and S.K. Antiochos, pp 129-142, AGU Geophysical Monograph 109, American Geophysical Union, Washington, 1999.

Schatten, K.H., J.M. Wilcox and N.F. Ness., A model of interplanetary and coronal magnetic fields, *Sol. Phys., 6*, 442-455, 1969.

Schlegel, K., G. Diendorfer, S. Thern, and M. Schmidt, Thunderstorms, lightening and solar activity – Middle Europe, *J. atmos. Sol-terr. Phys., 63*, 1705-1713, 2001.

Shindell, D.T., et al., Solar cycle variability, ozone and climate, *Science, 284*, 305, 1999.

Shindell, D.T., et al., Solar forcing of regional climate change during the Maunder minimum, *Science, 294*, 2149-2152, 2001.

Solanki , S.K. and M. Fligge, Solar irradiance since 1874 revisited, *Geophys. Res. Lett., 25*, 341-344, 1998.

Solanki, S.K. and M. Fligge, A reconstruction of total solar irradiance since 1700, *Geophys. Res. Lett., 26*, 2465-2468, 1999.

Solanki , S.K., M. Schüssler, and M. Fligge, Secular evolution of the Sun's magnetic field since the Maunder minimum, *Nature, 480*, 445-446, 2000.

Solanki , S.K., M. Schüssler, and M. Fligge, Secular evolution of the Sun's magnetic flux, *Astronomy and Astrophysics*, in press, 2001

Soon, W., S. Baluinas, E.S.Posmentier, and P. Okcke, Variations of solar coronal hole area and terrestrial lower tropospheric air temperature from 1979 to mid-1998: Astronomical forcings of changes in Earth's climate?, New Astron., *4*, 563-579, 2000.

Spruit, H.C., Theory of luminosity and radius variations, *in "The Sun in Time"*, eds. C.P. Sonnet, M.S. Giampapa and M.S.Matthews, Univ. of Arizona Press, pp. 118-159, ISBN 0-8165-1297-3, 1991.

Stamper, R., M. Lockwood, M.N. Wild, and T.D.G. Clark, Solar causes of the long term increase in geomagnetic activity, *J. Geophys Res., 104*, 28,325-28,342, 1999.

Stott, P. A., et al., External control of 20th c3entury temperature by natural and anthropogenic forcings, *Science, 290*, 2133-2137, 2000

Stuiver, M., and P.D. Quay, Changes in atmospheric carbon-14 attributed to a variable Sun, *Science, 207*, 11, 1980.

Suess, S.T., and E.J. Smith, Latitudinal dependence of the radial IMF component – coronal imprint, *Geophys. Res. Lett., 23*, 3267-3270, 1996.

Suess, S.T., et al., Latitudinal dependence of the radial IMF component – interplanetary imprint, *Astronomy and Astrophysics, 316*, 304-312, 1996.

Svensmark, H., and E. Friis-Christensen, Variation of cosmic ray flux and global cloud coverage: A missing link in solar-climate relationships, *J. Atmos. Sol. Terr. Phys., 59*, 1225-1232, 1997.

Svensmark, H., Influence of cosmic rays on Earth's climate, *Phys. Rev. Lett., 81*, 5027-5030, 1998.

Tett, S. F. B, et al., Causes of twentieth century temperature change near the Earth's surface. *Nature, 399*, 569-572, 1999.

Udelhofen, P.M., and R.D. Cess, Cloud cover variations over the United States: an influence of cosmic rays or solar variability, Geophys. Res. Lett., 28, 2617-2620, 2001.

Vasyliunas, V.M, et al., Scaling relations governing magnetospheric energy transfer, *Planet Space Sci., 30*, 359-365, 1982.

Wang, Y.-M., N.R. Sheeley Jr., and J. Lean, Understanding the evolution of Sun's magnetic flux, *Geophys. Res. Lett., 27*, 621-624, 2000a.

Wang , Y.-M., J. Lean, and N.R. Sheeley Jr., The long-term evolution of the Sun's open magnetic flux, *Geophys. Res. Lett., 27*, 505-508, 2000b.

Wang, Y.-M. and N.R. Sheeley Jr., Solar implications of Ulysses interplanetary field measurements, *Astrophys. J., 447*, L143-L146, 1995.

Wang , Y.-M., and N.R. Sheeley Jr., *J. geophys. Res.*, in press, 2002.

White, W. B. and Cayan, D. R., Quasi-periodicity and global symmetries in interdecadal upper ocean temperature varibility. *J. Geophys. Res.*, *103*, 21355-21354, 1998

White, W. B., Lean, J., Cayan, D. R. and Dettinger, M. D. Response of global upper ocean temperature to changing solar irradiance. *J. Geophys. Res.*, *102*, 3255-3266, 1997

Wigley, T.M.L. and S.C.B. Raper, Climatic change due to solar irradiance changes, *Geophys. Res. Lett.*, *17*, 2169-2172, 1990.

Willson, R.C., Total solar irradiance trend during cycles 21 and 22, *Science, 277*, 1963-1965, 1997.

Yu, F., and Turco, R. P., Ultrafine Aerosol Formation via Ion-Mediated Nucleation, *Geophys. Res. Lett.*, *27*, 883-886, 2000.

M. Lockwood, World Data Centre C-1 for Solar-Terrestrial Physics, Space Science Department, Rutherford Appleton Laboratory, Chilton, Didcot, Oxfordshire OX11 0QX, England, U.K. (m.lockwood@rl.ac.uk)